

Decomposition reaction of phosphate rock under the action of microwave plasma_

Hui Zheng(郑慧), Meng Yang(杨猛), Cheng-Fa Jiang(江成发)†, and Dai-Jun Liu(刘代俊)‡

Citation: Chin. Phys. B, 2021, 30 (**4**): 045201. DOI: 10.1088/1674-1056/abccb6
Journal homepage: http://cpb.iphy.ac.cn; http://iopscience.iop.org/cpb

What follows is a list of articles you may be interested in

Similarity principle of microwave argon plasma at low pressure

Xiao-Yu Han(韩晓宇), Jun-Hong Wang(王均宏), Mei-E Chen(陈美娥), Zhan Zhang(张展), Zheng Li(李铮), Yu-Jian Li(李雨键)

Chin. Phys. B, 2018, 27 (**8**): 085206. DOI: 10.1088/1674-1056/27/8/085206

Understanding hydrogen plasma processes based on the diagnostic results of 2.45 GHz ECRIS at Peking University

Wen-Bin Wu(武文斌), Hai-Tao Ren(任海涛), Shi-Xiang Peng(彭士香), Yuan Xu(徐源), Jia-Mei Wen(温佳美), Jiang Sun(孙江), Ai-Lin Zhang(张艾霖), Tao Zhang(张滔), Jing-Feng Zhang(张景丰), Jia-Er Chen(陈佳洱)

Chin. Phys. B, 2017, 26 (**9**): 095204. DOI: 10.1088/1674-1056/26/9/095204

Electrical and optical characteristics of the radio frequency surface dielectric barrier discharge plasma actuation

Wei-Long Wang(王蔚龙), Hui-Min Song(宋慧敏), Jun Li(李军), Min Jia(贾敏), Yun Wu(吴云), Di Jin(金迪)

Chin. Phys. B, 2016, 25 (**4**): 045203. DOI: 10.1088/1674-1056/25/4/045203

Spectral and ion emission features of laser-produced Sn and SnO_2 plasmas

Hui Lan(兰慧), Xin-Bing Wang(王新兵), Du-Luo Zuo(左都罗)

Chin. Phys. B, 2016, 25 (**3**): 035202. DOI: 10.1088/1674-1056/25/3/035202

Pulsed microwave-driven argon plasma jet with distinctive plume patterns resonantly excited by surface plasmon polaritons

Chen Zhao-Quan, Yin Zhi-Xiang, Xia Guang-Qing, Hong Ling-Li, Hu Ye-Lin, Liu Ming-Hai, Hu Xi-Wei, A. A. Kudryavtsev

Chin. Phys. B, 2015, 24 (**2**): 025203. DOI: 10.1088/1674-1056/24/2/025203

Decomposition reaction of phosphate rock under the action of microwave plasma*

Hui Zheng(郑慧), Meng Yang(杨猛), Cheng-Fa Jiang(江成发)†, and Dai-Jun Liu(刘代俊)‡

Department of Chemical Engineering, Sichuan University, Chengdu 610065, *China*

(Received 27 September 2020; revised manuscript received 6 November 2020; accepted manuscript online 23 November 2020)

The decomposition reaction of phosphate rock under the action of microwave plasma was investigated. Phosphate rock and its decomposition products were characterized by x-ray diffraction (XRD), energy disperse spectroscopy (EDS), and chemical analysis. The measurements of electron temperature (T_e) and electron density (N_e) of plasma plume under atmospheric pressure were carried out using optical emission spectroscopy(OES). The electron temperature (T_e) was determined based on the calculation of the relative intensity of the O II (301.91 nm) and O II (347.49 nm) spectral lines. Correspondingly, electron densities were obtained using the Saha ionization equation which was based on the C I (247.86 nm) line and the C II (296.62 nm) line under the assumption of local thermodynamic equilibrium (LTE). The relationship between the relative intensity of the active components and the gas output was studied by the spectrometer. Finally the reaction mechanism of the decomposition of the phosphate rock under the action of the atmospheric pressure microwave plasma was proposed. The results showed that with the increase of CO flow and microwave power, the electron temperature and electron density in the plasma show a decreasing and increasing trend. The CO is dissociated into gaseous carbon ions under the action of microwave plasma, and the presence of gaseous carbon ions promotes the decomposition of the phosphate rock.

Keywords: microwave plasma, phosphorus decomposition, optical emission spectroscopy, reaction mechanism

PACS: 52.40.Hf, 82.33.Xj, 82.60.–s **DOI:** 10.1088/1674-1056/abccb6

1. Introduction

Phosphorus is an important raw material for the production of fine phosphorous chemicals and high-quality phosphoric acid. The production source of yellow phosphorous is mainly derived from the decomposition of phosphate rock. Although there are many reserves of phosphate ore resources in the world, there are few rich mines. This requires the development of production technologies that can make good use of low-grade refractory phosphate rock.

At present, the yellow phosphorus production industry mainly adopts the electric furnace method. This method has the advantages of good product quality (purity can reach 99.9%), high labor productivity, and low cost. But it consumes a lot of energy. The operating temperature is around 1600 K. For every 1 t of yellow phosphorus produced, it takes about 10 t of phosphate ore, electricity consumption is about 1.3×10^4 kW·h to 1.5×10^4 kW·h, and slag discharge is 9 t to 11 t. In addition, electric furnace method seriously pollute the environment and is not in line with current green development needs. Therefore, the development of energy-saving and consumption-reducing, clean production technology of yellow phosphorus production is of great significance to the sustainable development.

In recent years, the research and application of microwave plasma technology has shown an obvious upward trend. Microwave plasma technology is to convert microwave energy into the internal energy of gas molecules, so that it can be excited, dissociated, and ionized into active species. Compared with dielectric barrier discharge, direct current arc, and radio frequency plasma, microwave plasma has the advantages of no electrode pollution, high purity, high energy utilization, high electron density, and uniform plasma distribution. This makes it have practical application value and wide application prospects. Microwave plasma can be used in many fields, such as sputtering film formation,[1] plasma chemical vapor deposition (PCVD),[2] plasma polymerization, and initiation polymerization,[3] surface modification of materials,[4] *etc*.

Spectroscopic diagnosis of microwave plasma characteristics under atmospheric pressure is very important for the understanding of the reaction mechanism. Electron temperature (T_e) and electron density (N_e) are important parameters of plasma, and they have an important influence on the application of plasma.[5] Optical emission spectroscopy (OES) was usually used to diagnose plasmas, it can provide a lot of information about plasma species. Using this method, some basic characteristics of the plasma can be obtained by recording the emission intensity of different excited states to obtain the electron temperature,[6,7] or the electron density can be measured by obvious broadening of the spectral line.[8] Because

*Project supported by the National Natural Science Foundation of China (Grant No. 21076131).

†Corresponding author. E-mail: jiangcf@scu.edu.cn

‡Corresponding author. E-mail: liudj721@163.com

© 2021 Chinese Physical Society and IOP Publishing Ltd

there are many excited atoms and free radicals in the plasma, they directly or indirectly participate in plasma chemical reaction processes and affect the decomposition and formation of substances in the plasma. The plasma species information obtained by OES can be used to explore the chemical reactions occuring in the plasma and help to understand the reaction mechanism.

Up to now, there have been few reports about the decomposition phenomenon of phosphate rock under the action of microwave plasma. In this paper, we mainly study the reaction mechanism of the decomposition of low-grade phosphate rock under the action of atmospheric pressure microwave plasma. In experiment, the phosphate rock and its decomposition products are characterized by x-ray diffraction (XRD) techniques, energy disperse spectroscopy (EDS), and chemical method. At the same time, the plasma emission spectroscopy is used to study the characteristics of atmospheric pressure microwave plasma, to investigate and determine the electron temperature (T_e) and electron density (N_e) of the plasma, clarify the composition of free radicals in atmospheric pressure microwave plasma, and obtain the reaction mechanism of the phosphate rock decomposition under the action of atmospheric pressure microwave plasma.

2. Experiment

The phosphate rock is from a factory in Sichuan, China. The minerals are analyzed by ICP-AES and chemical method, volumetric method, and other methods. The main chemical components are shown in Table 1. The powdered activated carbon with analytical grade (AR) is used as the reducing agent.

The self-developed compressed waveguide microwave plasma device is used as the experimental equipment. Its microwave frequency is 2.45 GHz and the output power is adjustable from 0 W to 1300 W. The device is mainly composed of a microwave generator, a reaction chamber, a vacuum system, a cooling system and an air intake control system. The cooling system adopts circulating water cooling, and the intake air flow is controlled by a rotameter, as shown in Fig. 1. Multi-channel high-resolution plasma dedicated analysis photoelectric acquisition system spectrometer (AVANTES B.V. AvaSpecULS2048-4-USB2-RM) is used for spectrum measurement. This spectrometer uses a fiber optic detector, the best optical resolution can reach 0.10 nm, and the measurement spectrum band range is 180 nm–710 nm.

Table 1. Chemical composition of raw phosphate rock.

Oxides	Oxides in phosphate rock						
	P_2O_5	CaO	MgO	K_2O	Fe_2O_3	F	Other
wt%	22.48	32.06	3.00	3.37	7.07	2.48	29.54

In the experiment, a certain amount of phosphate rock with a particle size of 120 meshes was mixed with activated carbon in a certain proportion, then water was added to mix well (10% of water), and the tablets were dried. Put the compressed mixture into a graphite crucible, and carry out a reduction reaction under the action of microwave plasma. The experiment mainly investigates the influence of different reaction times. The phosphorus content in the product is determined in accordance with GB/T 1871.1-1995 "Determination of phosphorus pentoxide content in phosphate rock and phosphate concentrate-quinoline phosphomolybdate gravimetric method". The calcium content is determined in accordance with GB/T 1871.4-1995 "Determination of calcium oxide content in phosphate rock and phosphate concentrate volumetric method".

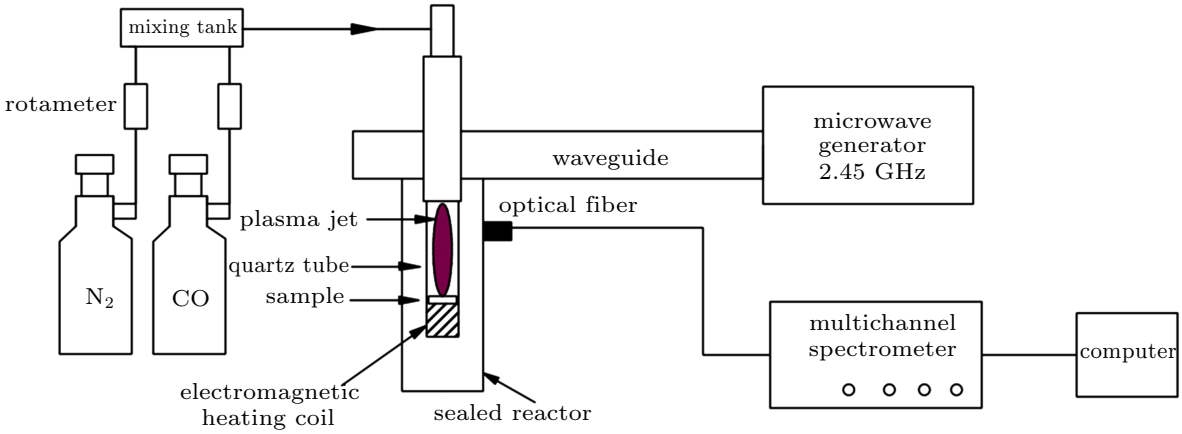


Fig. 1. Schematic diagram of the experimental set up.

Turn on successively the water cooling system, the microwave plasma equipment, the gas source, and adjust the power. A certain flow of working gas reaches the nozzle through the plasma resonance cavity. When the microwave power is large enough, the microwave energy at the tip of the nozzle can excite the gas discharge in the area to form a plasma jet. The optical fiber probe of the spectrometer is aimed at the center of the plasma flame to record the plasma spectrum data

in time. N_2 as the working gas and CO as the reducing gas were used in the experiment. The operating parameters for the experiments are given in Table 2. The experimental raw materials and products are tested and characterized by XRD, EDS, chemical analysis, and other technologies.

Table 2. Experimental operating parameters.

Input power (W)	1300
Plasma gas and flow rate	nitrogen; 2.5 L/min
Reducing gas and flow rate	carbon monoxide; 0.6 L/min
Reaction feedstock	M(phosphorite):M(acticarbon)=1:6
Processing time (min)	5/10/15/20
Plasma flame height (cm)	5.5
Graphite base temperature (°C)	800±15
Plasma temperature (K)	1200±20

3. Results and discussion

3.1. Thermodynamic analysis of phosphate rock decomposition

The change of Gibbs free energy is the only criterion for judging whether a chemical reaction can occur. This reaction can occur only when the Gibbs free energy of the reaction is less than zero. Phosphorus in phosphate rock is in the form of $Ca_5(PO_4)_3F$, so the process of extracting phosphorus from the phosphate rock is actually the reduction process of $Ca_5(PO_4)_3F$. When carbon and carbon monoxide are used as reducing agents, the most likely chemical reaction formulas for the phosphate rock decomposition are shown below:[9]

$$2Ca_5(PO_4)_3F + 15C(s) = 3P_2(g) + 15CO(g) + 9CaO + CaF_2, \quad (1)$$

$$4Ca_5(PO_4)_3F + 30C(s) + 9SiO_2 = 6P_2(g) + 30CO(g) + 9CaO + 9CaSiO_3 + 2CaF_2, \quad (2)$$

$$2Ca_5(PO_4)_3F + 15C(s) + 9SiO_2 = 3P_2(g) + 15CO(g) + 9CaSiO_3 + CaF_2, \quad (3)$$

$$2Ca_5(PO_4)_3F + 15CO(g) = 3P_2(g) + 15CO_2(g) + 9CaO + CaF_2, \quad (4)$$

$$4Ca_5(PO_4)_3F + 30CO(g) + 9SiO_2 = 6P_2(g) + 30CO_2(g) + 9CaO + 9CaSiO_3 + 2CaF_2, \quad (5)$$

$$2Ca_5(PO_4)_3F + 15CO(g) + 9SiO_2 = 3P_2(g) + 15CO_2(g) + 9CaSiO_3 + CaF_2. \quad (6)$$

The HSC Chemistry 6.0 software is used to calculate the Gibbs free energy change (ΔG) of the above reactions with temperature (T). The calculation results are shown in Fig. 2.

From Fig. 2, it can be seen that when C(s) is used as the reducing agent, the corresponding temperatures when $\Delta G = 0$ in Eqs. (1)–(3) are 1808 K, 1670 K, and 1533 K, respectively. When CO is the reducing agent, the corresponding temperatures when $\Delta G = 0$ in Eqs. (4)–(6) are 5204 K, 4975 K, and 4653 K, respectively. It can be seen that when carbon and carbon monoxide are used as reducing agents, the minimum temperature of the phosphate rock decomposition is relatively high. If C(g) is used as the reducing agent, the chemical reaction formula of phosphate rock decomposition is[9]

$$2Ca_5(PO_4)_3F + 15C(g) = 3P_2(g) + 15CO(g) + 9CaO + CaF_2, \quad (7)$$

$$4Ca_5(PO_4)_3F + 30C(g) + 9SiO_2 = 6P_2(g) + 30CO(g) + 9CaO + 9CaSiO_3 + 2CaF_2, \quad (8)$$

$$2Ca_5(PO_4)_3F + 15C(g) + 9SiO_2 = 3P_2(g) + 15CO(g) + 9CaSiO_3 + CaF_2. \quad (9)$$

Figure 2(c) shows the Gibbs free energy change (ΔG, kJ·mol^{-1}) with temperature (T, K) calculated by the HSC Chemistry 6.0 software from Eqs. (7)–(9). From Fig. 2(c), it can be seen that when the phosphate rock reacts with C(g), the lowest temperature of the reaction is much less than 100 K, so an attempt can be made to reduce the phosphate rock under the condition of C(g).

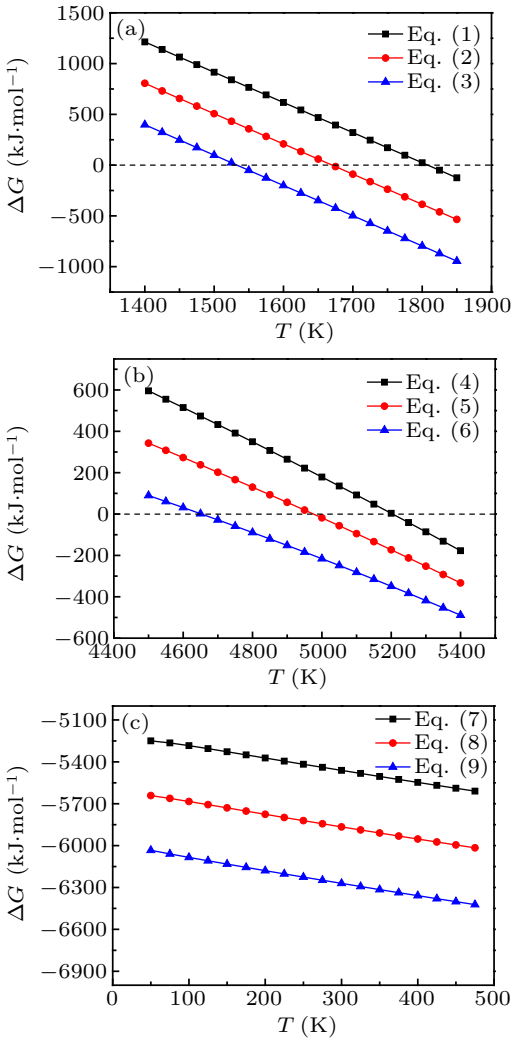


Fig. 2. Profiles of ΔG–T from chemical reaction equations: (a) Eqs. (1)–(3); (b) Eqs. (4)–(6); and (c) Eqs. (7)–(9).

LD Pietanza *et al.*[10] studied the non-equilibrium plasma kinetics of CO reaction under microwave discharge conditions. It was found that under the conditions of microwave discharge, CO follows a pure vibration mechanism, that is, CO can dissociate directly from CO+M→C+O+M, the ionization energy is 11.128 eV. At the same time, under the collision of electrons, CO ionizes in the following way, namely, e+CO←→e+CO^++e, CO^++e→C^+O. From this we know that C(g) can be obtained from the dissociation of oxygen-containing gas in microwave plasma. Therefore in the present work, CO is applied as the working gas to reduce the phosphate rock under the action of microwave plasma.

3.2. Phosphate rock decomposition

The XRD pattern of the raw phosphorus powder is shown in Fig. 3. Figure 4(a) shows the XRD patterns of phosphate rock reduction under microwave plasma at different reaction times. Figure 4(b) shows the intensity changes of the diffraction peaks of Ca_2SiO_4 and $CaSiO_3$ at different reaction times. It can be seen from these figures that, when the phosphate rock is reduced under the action of plasma, two diffraction peaks of Ca_2SiO_4 and $CaSiO_3$ appear in the XRD pattern of the product, indicating that the phosphate rock reacts with CO to form Ca_2SiO_4 and $CaSiO_3$. As the reaction time increases, the intensity of the $CaSiO_3$ diffraction peak first increases and then decreases, while the intensity of the Ca_2SiO_4 diffraction peak basically remains unchanged. It can be known that when the reaction time is 10 min, the output of $CaSiO_3$ is the highest.

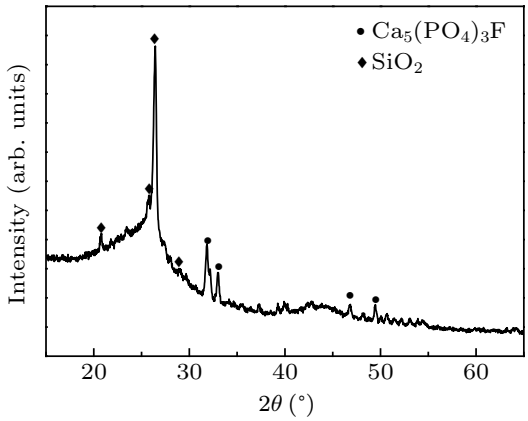


Fig. 3. XRD pattern of raw phosphorus powder.

The EDX spectrum of the phosphate rock decomposed under the action of microwave plasma is shown in Fig. 5. P, Ca, Si, and oxygen peaks are clearly identified. The EDX spectrum shows that the P peak is attenuated more than the Ca peak after the phosphate rock reacts for 10 min, indicating that the phosphate rock has decomposed during this process. Therefore, it can be seen from the EDX spectrum that the phosphate rock undergoes a decomposition reaction under the action of microwave plasma.

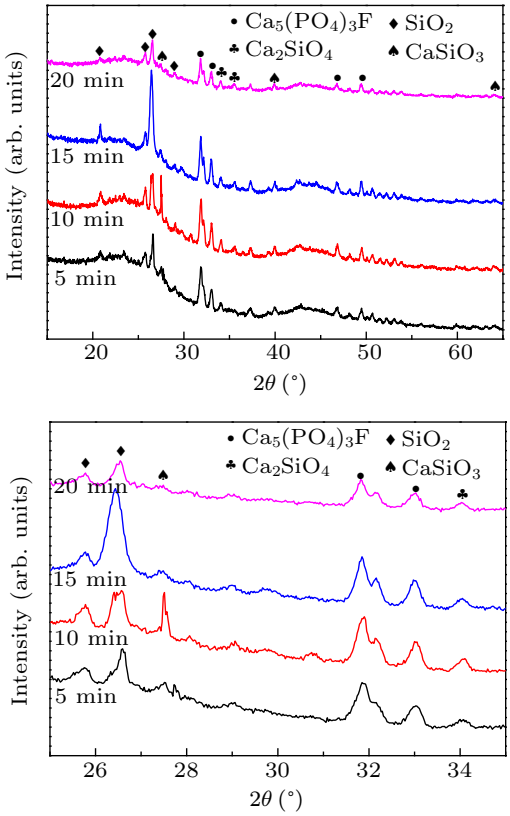


Fig. 4. XRD pattern of microwave plasma dissociated phosphorus at different times.

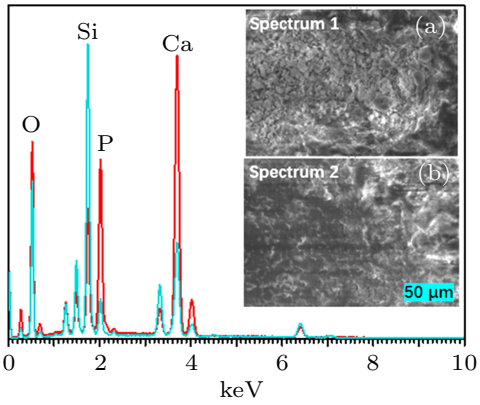


Fig. 5. EDS spectrum of phosphate rock decomposition under microwave plasma: (a) before the phosphate rock decomposes (b) after the phosphate rock is decomposed.

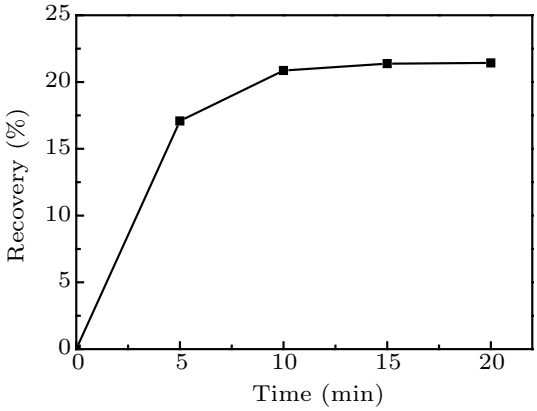


Fig. 6. The relationship between the reaction time and the conversion rate of phosphate rock.

Figure 6 shows the relationship between the reaction time and the conversion rate of the phosphate rock. From Fig. 6, it can be seen that the phosphate rock has a certain conversion rate under the action of microwave plasma, and as the reaction time increases, the reduction rate of the phosphate rock shows a slow upward trend. According to the experimental results, we can infer that the phosphate rock reduction reaction is completed in a short time under the action of microwave plasma, and a too long reaction time is meaningless to the phosphate rock reduction reaction.

The above results confirmed that the phosphate rock had a decomposition reaction under the action of microwave plasma. The main products are Ca_2SiO_4 and $CaSiO_3$. It can be inferred that certain active particles excited by the microwave plasma promote the decomposition of the phosphate rock. The plasma emission spectroscopy is used to determine the excited atoms and free radicals participating in the decomposition reaction.

3.3. Spectral diagnosis of microwave plasma characteristics

There are many excited atoms and free radicals in the plasma. They participate in the plasma chemical reaction and affect the decomposition and generation of substances in the plasma. At the same time, electrons dominate the plasma ionization and collision between particles. Electron temperature (T_e) and electron density (N_e) are the most important physical parameters that characterize the plasma state. Only by spectral diagnosis of atmospheric pressure microwave plasma can we understand the composition of excited atoms and free radicals inside the plasma, calculate the electron temperature and electron density, and infer the surface decomposition reaction mechanism of the phosphate rock under the action of microwave plasma.

In this paper, the electron temperature (T_e) of the plasma is measured by the relative intensity of the ion emission line. For the relative intensity ratio of two O II spectral lines, the intensity measurement of spectral lines emitted by the plasma jet, when the assumption of LTE is made, is given by[11]

$$I_{ik} = \frac{1}{4\pi}\frac{N}{Z}\frac{hc}{\lambda}A_{ik}g_i\exp\left(-\frac{E_i}{kT}\right), \tag{10}$$

where λ is the emission spectrum wavelength; h is the Planck constant, 6.626×10^{-34} J·s; c is the speed of light, 3×10^{-8} m·s^{-1}; k is the Boltzmann constant, 1.38065×10^{-23} J·K^{-1}; N is the layout density of the ground state energy; Z is the partition function. The subscripts i and k are the main quantum numbers corresponding to the upper and lower levels of the line; E_i is the energy of the corresponding level; g_i is the statistical weight of the energy level; and A_{ik} is the spontaneous transition probability from level i to level k. Therefore, the electron temperature (T_e) can be obtained by using the intensity of two spectral lines with the same ionization state of the same element. The final formula for the electron temperature is given by:

$$T_e = \frac{1}{k}(E_k - E_i)\left(\ln\frac{I_i g_k \upsilon_k A_k}{I_k g_i \upsilon_i A_i}\right)^{-1}, \tag{11}$$

when v is the emission frequency.

Under LTE conditions, the electron density (N_e) can be obtained by using the Saha ionization equation[12]

$$N_e = 2\frac{I_{ik}^Z g_i^{Z+1}\upsilon_{ik}^{Z+1}A_{ik}^{Z+1}}{I_{ik}^{Z+1}g_i^Z\upsilon_{ik}^Z A_i^Z}\cdot\left(\frac{2\pi m_e kT_e}{h}\right)^{3/2} \times\exp\left(\frac{E^Z - E^{Z+1} - E_\infty^Z}{kT_e}\right). \tag{12}$$

Here, Z and $Z+1$ represent two adjacent ionization states of the same element; m_e is electron mass, 9.11×10^{-31} kg; E_∞ is the ionization energy of Z ionized particles. In this study, the intensity of the two spectral lines O II (301.91 nm) and O II (347.49 nm) were used to calculate the electron temperature, and the intensity of the C I (247.86 nm) and C II (296.62 nm) lines is used to calculate the electron density. The Kurucz database will be used to identify the spectral lines of these elements.[13]

The experiment investigated the influence of CO variable and microwave power on electron temperature and electron density. A typical spectral emission at 1300 W and N_2/CO flow rate 3/0.6 L/min is shown in Fig. 7.

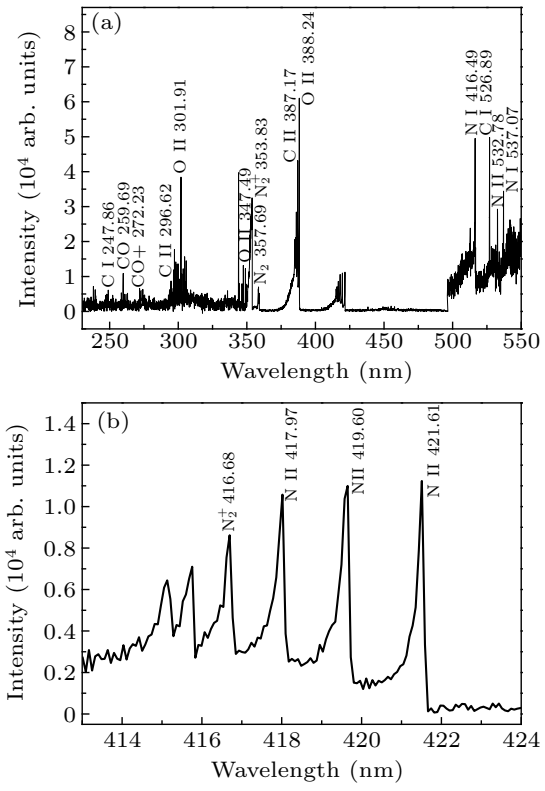


Fig. 7. Typical spectral emission at 1300 W and N_2/CO flow rate 3/0.6 L/min: (a) wavelength from 230 nm to 550 nm; (b) wavelength from 413 nm to 424 nm.

The spectrum shows that the groups that may exist under the action of microwave plasma are CO, CO^+, C I, C II, O II, N_2, N_2^+, N I, N II. Among them, CO and N_2 represent excited carbon monoxide molecules and nitrogen molecules; CO^+, N_2^+ represent excited carbon monoxide charged particles and nitrogen charged particles; C I, NI represent excited neutral carbon atoms and neutral nitrogen atoms; C II, O II and N II represent the excited state carbon ions, oxygen ions, and nitrogen ions. The spectral information of C I, C II, and O II are listed in Table 3. Table 3 shows the λ, A_{ik}, E, and g_i values of each element.

Table 3. Species and wavelengths used in measurements.

Element	λ (nm)	A_{ik} (s^{-1})	E (eV)	g_i
O II	301.91	1.75×10^7	32.96	2
O II	347.49	8.53×10^5	28.85	2
C I	247.86	1.80×10^7	7.68	3
C II	296.62	7.54×10^6	27.29	4

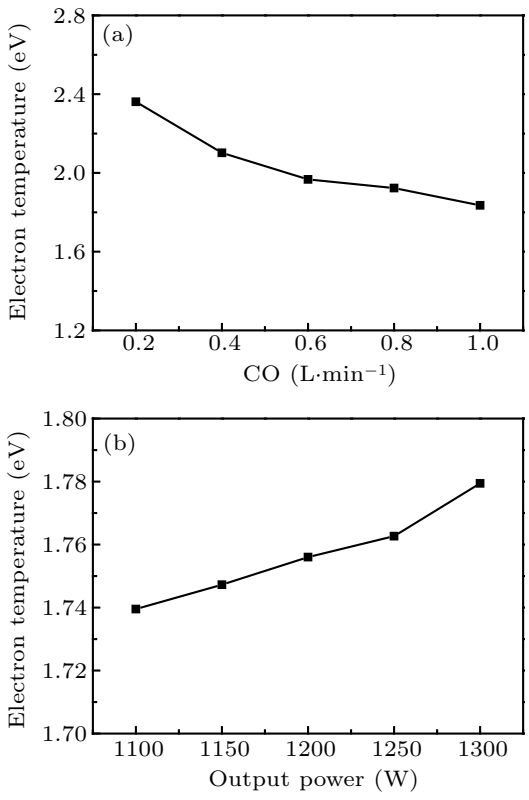


Fig. 8. The variations of electron temperature with different CO flows and different microwave output powers.

According to formulas (10)–(13) and the elemental spectrum data in Table 3, the electron temperature can be obtained under different CO flows and microwave powers, as shown in Fig. 8. As the CO flow rate and microwave output power increase, the electron temperature changes significantly. The electron temperature is an important parameter to determine the kinetic energy of electrons in plasma. Figure 8(a) shows that as the CO flow rate increases, the electron temperature shows a downward trend. This is because when the output power is constant, the increase of CO flow requires more energy for the dissociation of CO, while the constant microwave power makes the energy input in the plasma constant, and the kinetic energy of electrons will decrease. Figure 8(b) shows that as the microwave input power increases, the electron temperature increases slightly, but the increase is not significant. The CO flow rate remains unchanged, and the increase of input energy will inevitably cause the increase of the content of excited state particles produced by dissociation. The reason for the insignificant increase is because, in the spectrum obtained according to different output powers, the intensity of the CO^+ spectrum shows an insignificant increase as the power increases. That is, there is no obvious change in the average kinetic energy of electrons, so that there is no obvious change in the types of excited particles produced by the electron excitation and dissociation processes of the CO molecules.

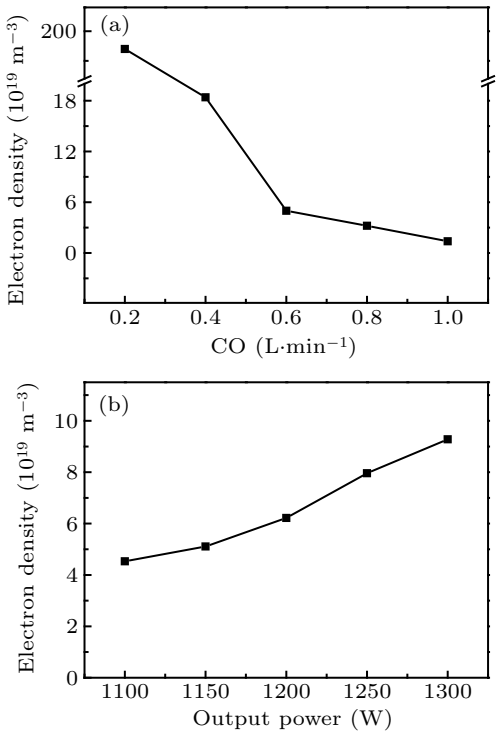


Fig. 9. the variation in the electron temperature with the different CO flows and different microwave output power.

Figure 9 shows the changing trend of electron density under different CO flows and microwave powers. The numerical value of the electron density can indicate the concentration of electrons in the plasma. Figure 9(a) shows that as the CO flow increases, the electron density decreases. The increase of CO flow makes the dissociation of CO require more energies, and the constant microwave power ensures that the input energy remains unchanged, and the energy is not enough to supply the energy required for CO dissociation or recombination, so the electron concentration will decrease with the increase of the CO flow. It can be seen from Fig. 9(b) that as the output power

increases, the electron density shows a clear upward trend. The flow of CO and nitrogen remains constant, the temperature of electrons changes little, and the average kinetic energy of electrons remains unchanged. The input energy continues to increase, and the dissociation of CO gets a sufficient energy supply. The content of excited particles produced by dissociation is increasing, that is, the electron concentration increases. This is similar to the results reported in the literature.[14]

3.4. The mechanism of the decomposition of phosphate rock under the action of microwave plasma

According to the relationship between the relative intensity of the active particles and the gas production in the spectrum shown in Fig. 7, it can be seen that the spectral peaks of C I, C II, and O II are relatively strong. CO can dissociate from $CO \rightarrow C(^3P) + O(^3P)$, the dissociation energy of is 11.128 eV. CO molecule has 80 vibrational levels in the ground electronic state, and there are several electronic excited states at the same time, namely three triplet states, $a^3\Pi$(6.01 eV), $a^3\Sigma^+$(6.86 eV), $b^3\Sigma^+$(10.40 eV) and four singlet states, $A^1\Pi$(8.03 eV), $B^1\Sigma^+$(10.78 eV), $C^1\Sigma^+$(11.40 eV), $E^1\Sigma^+$(11.52 eV). For C and O atoms, they have four and five electronic energy levels respectively, namely, $C(^3P)$, $C(^1D)$, $C(^1S)$, $C(^5S^0)$, and $O(^3P)$, $O(^1D)$, $O(^1S)$, $O(^3S^0)$, $O(^5S^0)$. The excitation potentials of CO^+, C^+, and O^+ are 14.01 eV, 11.26 eV, and 13.61 eV, respectively. Their energies have been taken from the Kurucz database. For all the plasma species (CO, C, O, CO^+, C^+, O^+) momentum transfer cross sections (MT), taken mainly from the LXcat database.[15]

Therefore, we can infer the mechanism of phosphate rock decomposition under microwave plasma:.[10,16–20]

(i) CO decomposition

$$CO + e \rightarrow CO^+ + 2e, \tag{13}$$

$$CO + e \rightarrow C + O + e, \tag{14}$$

$$CO^+ + e \rightarrow C + O, \tag{15}$$

$$O + e \rightarrow O^+ + 2e, \tag{16}$$

$$C + e \rightarrow C^+ + 2e, \tag{17}$$

(ii) recombination reaction

$$CO + O \rightarrow CO_2, \tag{18}$$

$$CO + O^+ + e \rightarrow CO_2, \tag{19}$$

$$CO_2 + C \rightarrow CO, \tag{20}$$

$$CO_2 + C^+ + e \rightarrow CO, \tag{21}$$

$$CO(v) + CO(w) \rightarrow CO_2 + C, \tag{22}$$

(iii) C(g) reacts with phosphate rock

$$Ca_5(PO_4)_3F \rightarrow Ca_3(PO_4)_2 + CaF_2, \tag{23}$$

$$Ca_3(PO_4)_2 + C(g) + SiO_2 \rightarrow CaSiO_3 + P_2(g) + CO(g), \tag{24}$$

$$Ca_3(PO_4)_2 + C(g) + SiO_2 \rightarrow Ca_2SiO_4 + P_2(g) + CO(g). \tag{25}$$

$$CaSiO_3 + CaO \rightarrow Ca_2SiO_4. \tag{26}$$

Among them, CO(v) and CO(w) represent CO molecules at v and w energy levels, and they may combine to generate CO_2 and C. Because the intensity of the O II line in the spectrum is relatively high. The P_2 produced by the decomposition of phosphate rock may combine with O or O^+ separated from CO to form phosphorus oxides, which is also the reason for the low conversion rate of phosphate rock.

4. Conclusions

In the present work, we confirm that the decomposition reaction occurs in phosphate rock under the action of microwave plasma. At the same time, plasma optical emission spectroscopy (OES) is used to study the characteristics of atmospheric pressure microwave plasma, and the electron temperature (T_e) and electron density (N_e) of the plasma are investigated and measured. The results show that with the increase of CO flow and microwave power, the electron temperature and electron density in the plasma show a decreasing and increasing trend, which has an important relationship with the energy required for CO dissociation and recombination. The experiment also determined the composition of free radicals in atmospheric pressure microwave plasma through the full spectrum was studied by spectroscopy. According to the relationship between the relative intensity of the active particles and the gas production, we obtained the reaction mechanism of phosphate rock decomposition under the action of atmospheric pressure microwave plasma.

It is known from the reaction mechanism that CO decomposes gaseous carbon ions under the action of microwave power, and the presence of gaseous carbon ions promotes the decomposition of phosphate rock. This shows that the application of atmospheric pressure microwave plasma technology to extract phosphorus from phosphate rock has great development potential.

References

[1] Hao Q, Fu X H, Song S G, Gibson D, Li C, Chu H O and Shi Y J 2018 *Coatings* **8** 270
[2] Das D and Roy A 2020 *Appl. Surf. Sci.* **515** 146043
[3] Ibrahim N I and Wasfi A S 2019 *Synth. Met.* **250** 49
[4] Azahara A G, Enrique R C and David P M 2020 *Appl. Surf. Sci.* **513** 145764
[5] Chang Z S, Zhang G J, Shao X J and Zhang Z H 2012 *Phys. Plasmas* **19** 073513
[6] Mariotti D, Shimizu Y, Sasaki T and Koshizaki N 2007 *J. Appl. Phys.* **101** 013307
[7] Sarani A, Nikiforov A Y and Leys C 2010 *Phys. Plasmas* **17** 063504

[8] Holclajtner-Antunovic I, Raskovic M and Jovicevic S 2004 *Spectrochimica Acta Part B-Atomic Spectroscopy* **59** 419
[9] Liang J G, Wei T J and Yong L 2013 *Phosphate & Compound Fertilizer* **28** 15 (in Chinese)
[10] Pietanza L D, Colonna G and Capitelli M 2017 *Plasma Sources Sci. Technol.* **26** 125007
[11] Peters J, Bartlett B, Lindsay J and Heberlein J 2008 *Plasma Chem. Plasma Process.* **28** 331
[12] Sarkar A and Singh M 2017 *Plasma Sci. Technol.* **19** 025403
[13] Kurucz Atomic Database
[14] Ota K, Kato Y and Teii K 2019 *Jpn. J. Appl. Phys.* **58** 016003
[15] https://nl.lxcat.net/home/, LXcat database
[16] Laporta V, Tennyson J and Celiberto R 2016 *Plasma Sources Sci. Technol.* **25** 01
[17] Essenhigh K A, Utkin Y G, Bernard C, Adamovich I V and Rich J W 2006 *Chem. Phys.* **330** 506
[18] Plonjes E, Palm P, Chernukho A P, Adamovich I V and Rich J W 2000 *Chem. Phys.* **256** 315
[19] Shin D H, Hong Y C, Lee S J, Kim Y J, Cho C H, Ma S H, Chun S M, Lee B J and Uhm H S 2013 *Surf. Coat. Technol.* **228** 520
[20] Uhm H S, Na Y H, Hong Y C, Shin D H, Cho C H and Park Y K 2014 *Energy & Fuels* **28** 4402